Inorganic Chemistry
Article

Inorg. Chem. **2009**, *48*, 6781–6793 **6781**
DOI: 10.1021/ic9007608

Polynuclear Nickel(II) Complexes: A Magnetostructural Study of Ni^{II}_4, Ni^{II}_6, and Ni^{II}_9 Species with Oxime Ligands

Biplab Biswas, Ulrich Pieper, Thomas Weyhermüller, and Phalguni Chaudhuri*

Max-Planck-Institut für Bioanorganische Chemie, Stiftstrasse 34-36, D-45470 Mülheim an der Ruhr, Germany

Received April 20, 2009

Syntheses, crystal structures, and magnetic properties are reported for a tetrametallic (complex **1**), a nonametallic (complex **2**), and two hexametallic (complexes **3** and **4**) nickel(II) clusters, namely, $[Ni_4(HL^1)_2(\mu\text{-OAc})_2(MeOH)]$ (**1**), $[Ni_9(L^2)_{10}(\mu_3\text{-OH})_2(\mu\text{-OH})_2(\mu\text{-OH}_2)_2(OH_2)_6](ClO_4)_4$ (**2**), $[Ni_6(L^2)_9(L^2H)(MeOH)(H_2O)_2](ClO_4)_3$ (**3**), and $[Ni_6(L^3)_3(\mu_3\text{-O})_2](ClO_4)_2$ (**4**), where H_4L^1 represents N,N′-dimethyl-N,N′-ethylene-bis(5-bromo-3-formyloxime-2-hydroxybenzylamine); HL^2, 1-methylimidazole-2-aldoxime; and H_2L^3, N,N′-bis(2,3-butanedionemonoxime-2-ene)-3(aminomethyl)-benzylamine. The structure of **1** can be considered as two face-sharing bioctahedral units of $[Ni_2(\mu\text{-O}_{phen})_2(\mu\text{-OAc})]$ bridged by a two-atom (−N−O−) oximate linker. The $Ni^{II}\cdots Ni^{II}$ distances of av. 2.935 Å preclude metal−metal bonding, although they are remarkably short. Variable-temperature magnetic susceptibility data are fitted to obtain the parameters $J_1 = +8.0\ cm^{-1}$, $J_2 = -16.0\ cm^{-1}$, and $g = 2.19$ ($\hat{H} = -2\,JS_i \cdot S_j$). The ferromagnetic coupling J_1 operates between the nickel(II) centers in the face-sharing bioctahedral units, whereas J_2 represents the antiferromagnetic interactions mediated by a single (−N−O−) bridge separating the two nickel centers at a distance of ∼4.71 Å. A rationale for the disparate nature of interactions based on a comparison with those reported in the literature is forwarded. The structure of **2** consists of two $[Ni_4(L^2)_5]$ units linked covalently to a central nickel atom by four oximate and two hydroxy oxygen atoms, resulting in a central octahedral NiO_6 core and thus yielding the nonanuclear nickel(II) cluster. The magnetic data were analyzed by a "two-*J*" model, yielding pairwise antiferromagnetic exchange interactions, $J_1 = -24.0\ cm^{-1}$ and $J_2 = -5.8\ cm^{-1}$, between the nickel centers. The spin ground state of $S_t = 1.0$ has been confirmed by magnetization measurements (variable-temperature, variable-field) at different fields. The structure of **3** contains six nickel(II) centers, each of which is six-coordinated but with different coordination environments: NiN_6, NiO_6, NiN_3O_3(2×), NiN_4O_2, and $NiNO_5$. The ground-state spin has been observed to be S_t=1.0 with the axial zero-field splitting parameter $D = -7.2\ cm^{-1}$. Complex **4** is a rare example of dimeric $[Ni_3(\mu_3\text{-O})]^{4+}$ units, in which each of six nickel(II) centers is in square-planar geometry with low-spin d^8 Ni(II) centers, thus rendering diamagnetism to complex **4**.

Introduction

The study of polynuclear complexes of paramagnetic metal ions is of unabated interest to inorganic chemists, because of their relevance to bioinorganic chemistry[1−3] and molecular magnetic materials.[4−6] Control of magnetic interactions in polynuclear complexes is a key for building molecule-based magnets.[5] Despite the interest in the properties of such complexes, synthetic methods have yet to reach the level of efficiency attained with mononuclear complexes. Organic ligands play a central role in the successful preparation of polymetal complexes. Thus, the use of new ligands remains important in related fields. We are continuously using the strategy of "metal oximate" building blocks[7,8] as ligands to design and synthesize

*To whom correspondence should be addressed. E-mail: chaudh@mpi-muelheim.mpg.de.

(1) (a) Holm, R. H.; Solomon, E. I. *Chem. Rev.* **1996**, *96*, 7. (b) Holm, R. H.; Solomon, E. I. *Chem. Rev.* **2004**, *104*, 2.

(2) (a) Lippard, S. J.; Berg, J. M. *Principles of Bioinorganic Chemistry*; University Science Books: Mill Valley, CA, 1994. (b) Kaim, W.; Schwerderski, B. *Bioanorganische Chemie*; B. G. Teubner: Stuttgart, Germany, 1991. (c) Karlin, K. D.; Tyeklar, Z. *Bioinorganic Chemistry of Copper*; Chapman & Hall: New York, 1993.

(3) Messerschmidt, A.; Huber, R.; Poulos, T.; Wieghardt, K. *Handbook of Metalloproteins*; John Wiley & Sons: Chichester, UK, 2001.

(4) (a) Gatteschi, D.; Kahn, O.; Miller, J. S.; Palacio, F. *Magnetic Molecular Materials*; Kluwer Academic Publishers: Dordrecht, The Netherlands, 1991. (b) O'Connor, C. J. *Research Frontiers in Magnetochemistry*; World Scientific: Singapore, 1993. (c) *J. Solid State Chem.* **2001**, *159* (2), a tribute to Oliver Kahn.

(5) Kahn, O. *Molecular Magnetism*; VCH: Weinheim, Germany, 1993.

(6) (a) Gatteschi, D.; Sessoli, R. *Angew. Chem., Int. Ed.* **2003**, *42*, 268. (b) Christou, G.; Gatteschi, D.; Hendrickson, D. N.; Sessoli, R. *MRS Bull.* **2000**, 66.

(7) (a) Chaudhuri, P. *Coord. Chem. Rev.* **2003**, *243*, 143. (b) Chaudhuri, P. *Proc. Indian Acad. Sci. (Chem. Sci.)* **1999**, *111*, 397.

(8) Selected examples: (a) Bill, E.; Krebs, C.; Winter, M.; Gerdan, M.; Trautwein, A. X.; Flörke, U.; Haupt, H.-J.; Chaudhuri, P. *Chem.—Eur. J.* **1997**, *3*, 193. (b) Verani, C. N.; Bothe, E.; Burdinski, D.; Weyhermüller, T.; Flörke, U.; Chaudhuri, P. *Eur. J. Inorg. Chem.* **2001**, 2161. (c) Chaudhuri, P.; Rentschler, E.; Birkelbach, F.; Krebs, C.; Bill, E.; Weyhermüller, T.; Flörke, U. *Eur. J. Inorg. Chem.* **2003**, 541. (d) Chaudhuri, P.; Hess, M.; Weyhermüller, T.; Bill, E.; Haupt, H.-J.; Flörke, U. *Inorg. Chem. Commun.* **1998**, *1*, 39. (e) Chaudhuri, P.; Hess, M.; Rentschler, E.; Weyhermüller, T.; Flörke, U. *New J. Chem.* **1998**, 553. (f) Khanra, S.; Weyhermüller, T.; Bill, E.; Chaudhuri, P. *Inorg. Chem.* **2006**, *45*, 5911. (g) Khanra, S.; Weyhermüller, T.; Chaudhuri, P. *Dalton Trans.* **2007**, 4675. (h) Khanra, S.; Weyhermüller, T.; Chaudhuri, P. *Dalton Trans.* **2008**, 4885 and references cited therein.

Published on Web 06/24/2009

multinuclear complexes in a controlled fashion. The present work is a natural extension of our program on exchange-coupled polynuclear systems and deals specifically with the ligation property of the functionalized oximes (Scheme 1). Since nickel(II) is known to have a large single-ion zero-field splitting[9] and often gives rise to ferromagnetic coupling,[10] we have especially focused our attention on polynuclear nickel(II) complexes. Although polynuclear nickel(II) complexes containing up to four metal ions[10a,11,12] are numerous, assemblies with five, six, and more nickel(II) ions still are numbered.[13−15] We anticipated that the use of oximes listed in Scheme 1 in metal−oximate chemistry would yield products with multimetal centers,[14,15] and therefore we explored their use initially in nickel chemistry. In this paper, we report on the extension of our studies with oxime ligands and include the preparation and magnetochemical characterization of

$$[Ni^{II}_4(HL^1)_2(\mu\text{-}OAc)_2(MeOH)] \quad (1)$$

$$[Ni^{II}_9(L^2)_{10}(\mu_3\text{-}OH)_2(\mu\text{-}OH)_2(\mu\text{-}OH_2)_2(OH_2)_6](ClO_4)_4 \quad (2)$$

$$[Ni^{II}_6(L^2)_9(L^2H)(MeOH)(H_2O)_2](ClO_4)_3 \quad (3)$$

$$[Ni^{II}_6(L^3)_3(\mu_3\text{-}O)_2](ClO_4)_2 \quad (4)$$

where H_4L^1, HL^2, and H_2L^3 are different oximes depicted in Scheme 1.

As the ligand 1-methylimidazole-2-aldoxime (HL^2)[16,17] and pyridine-2-aldoxime (HPyA)[17−19] (Scheme 1) resemble

(9) (a) Boca, R. *Coord. Chem. Rev.* **2004**, *248*, 757. (b) Krzystek, J.; Ozarowski, A.; Telser, J. *Coord. Chem. Rev.* **2006**, *250*, 2308.

(10) See, for example: (a) Paine, T. K.; Rentschler, E.; Weyhermüller, T.; Chaudhuri, P. *Eur. J. Inorg. Chem.* **2003**, 3167. (b) Papatriantafyllopoulou, C.; Jones, L. F.; Nguyen, T.; Matamoros-Salvador, N.; Cunha-Silva, L.; Paz, F. A. A.; Rocha, J.; Evangelisti, M.; Brechin, E. K.; Perlepes, S. P. *Dalton Trans.* **2008**, 3153.

(11) Some recent examples: (a) Psomas, G.; Dendrinou-Samara, C.; Alexiou, M.; Tsohos, A.; Raptopoulou, C. P.; Terzis, A.; Kessissoglou, D. P. *Inorg. Chem.* **1998**, *37*, 6556. (b) Palvlishchuk, V. V.; Kolotilov, S. V.; Addison, A. W.; Prushan, M. J.; Schollmeyer, D.; Thompson, L. K.; Goreshnik, E. A. *Angew. Chem., Int. Ed.* **2001**, *40*, 4734. (c) Yang, E. C.; Wernsdorfer, W.; Zakharov, L. N.; Karaki, Y.; Yamaguchi, A.; Isidro, R. M.; Lu, G. D.; Wilson, S. A.; Rheingold, A. L.; Ishimoto, H.; Hendrickson, D. N. *Inorg. Chem.* **2006**, *45*, 529. (d) Lawrence, J.; Yang, E. C.; Edwards, R.; Olmstead, M. M.; Ramsey, C.; Dalal, N. S.; Gantzel, P. K.; Hill, S.; Hendrickson, D. N. *Inorg. Chem.* **2008**, *47*, 1965. (e) Papaefstathiou, G. S.; Escuer, A.; Mauter, F. A.; Raptopoulou, C.; Terzis, A.; Perlepes, S. P.; Vincente, R. *Eur. J. Inorg. Chem.* **2005**, 879. (f) Efthymiou, C. G.; Raptopoulou, C. P.; Terzis, A.; Boca, R.; Korabic, M.; Mrozinski, J.; Perlepes, S. P.; Bakalbasis, E. G. *Eur. J. Inorg. Chem.* **2006**, 2236. (g) Hudson, T. A.; Berry, K. J.; Moubaraki, B.; Murray, K. S.; Robson, R. *Inorg. Chem.* **2006**, *45*, 3549. (h) Kersting, B.; Steinfeld, G.; Siebert, D. *Chem.—Eur. J.* **2001**, *7*, 4253. (i) Hendrickson, D. N.; Yang, E.-C.; Isidro, R. M.; Kirman, C.; Lawrence, J.; Edwards, R. S.; Hill, S.; Yamaguchi, A.; Ishimoto, H.; Wernsdorfer, W.; Ramsey, C.; Dalal, N.; Olmstead, M. M. *Polyhedron* **2005**, *24*, 2280. (j) Siebert, A.; Boskovic, C.; Bircher, R.; Waldmann, O.; Ochsenbein, S. T.; Chaboussant, G.; Güdel, H. U.; Kirchner, N.; van Slageren, J.; Wernsdorfer, W.; Neels, A.; Stoeckli-Evans, H.; Janssen, S.; Juranyl, F.; Mutka, H. *Inorg. Chem.* **2005**, *44*, 4315. (k) Chaboussant, G.; Basler, R.; Güdel, H.-U.; Ochsenbein, S.; Parkin, A.; Parsons, S.; Rajaraman, G.; Sieber, A.; Smith, A. A.; Timco, G. A.; Winpenny, R. E. P. *Dalton Trans.* **2004**, 2758. (l) Moragues-Cánovas, M.; Helliwell, M.; Ricard, L.; Riviére, E.; Wernsdorfer, W.; Brechin, E.; Mallah, T. *Eur. J. Inorg. Chem.* **2004**, 2219. (m) Du, M.; Bu, X.-H.; Guo, Y.-M.; Zhang, L.; Liao, D.-Z.; Ribas, J. *Chem. Commun.* **2002**, 1478. (n) Escuer, A.; Vicente, R.; Kumar, S. B.; Mautner, F. A. *J. Chem. Soc., Dalton Trans.* **1998**, 3473. (o) Matthews, C. J.; Avery, K.; Xu, Z.; Thompson, L. K.; Zhao, L.; Miller, D. O.; Biradha, K.; Poirier, K.; Zaworotko, M. J.; Wilson, C.; Goeta, A. E.; Howard, J. A. K. *Inorg. Chem.* **1999**, *38*, 5266. (p) Karmakar, T. K.; Chandra, S. K.; Ribas, J.; Mostafa, G.; Lu, T. H.; Ghosh, B. K. *Chem. Commun.* **2002**, 2364. (q) Pavlishchuk, V. V.; Kolotilov, S. V.; Additon, A. W.; Prushan, M. J.; Schollmeyer, D.; Thompson, L. K.; Weyhermüller, T.; Goreshnik, E. A. *Dalton Trans.* **2003**, 1587. (r) Aromi, G.; Batsanov, A. S.; Christian, P.; Helliwell, M.; Roubeau, O.; Timco, G. A.; Winpenny, R. E. P. *Dalton Trans.* **2003**, 4466. (s) Clemente-Juan, J. M.; Chansou, B.; Donnadieu, B.; Tuchagues, J.-P. *Inorg. Chem.* **2000**, *39*, 5515. (t) Mukherjee, S.; Weyhermüller, T.; Bothe, E.; Wieghardt, K.; Chaudhuri, P. *Eur. J. Inorg. Chem.* **2003**, 863. (u) Koikawa, M.; Ohba, M.; Tokii, T. *Polyhedron* **2005**, *24*, 2257.

(12) (a) Andrew, J. E.; Blake, A. B. *J. Chem. Soc. A* **1969**, 1456. (b) Barnes, J. A.; Hatfield, W. E. *Inorg. Chem.* **1971**, *10*, 2355. (c) Bertrand, J. A.; Ginsberg, A. P.; Kaplan, R. I.; Kirkwood, C. E.; Martin, R. L.; Sherwood, R. C. *Inorg. Chem.* **1971**, *10*, 240. (d) Aurivillius, B. *Acta Chem. Scand. A* **1977**, *31*, 501. (e) Bertrand, J. A.; Marabella, C.; Vanderveer, D. G. *Inorg. Chim. Acta* **1978**, *26*, 113. (f) Gladfelter, W. L.; Lynch, M. W.; Schaefer, W. P.; Hendrickson, D. N.; Gray, H. B. *Inorg. Chem.* **1981**, *20*, 2390. (g) Boyd, P. D.W.; Martin, R. L.; Schwarzenbach, G. *Aust. J. Chem.* **1988**, *41*, 1499. (h) Ballester, L.; Coronado, E.; Gutiérrez, A.; Monge, A.; Perpinán, M. F.; Pinella, E.; Rico, T. *Inorg. Chem.* **1992**, *31*, 2053. (i) Atkins, A. J.; Blake, A. J.; Schröder, M. *J. Chem. Soc., Chem. Commun.* **1993**, 1662. (j) Halcrow, M. A.; Sun, J.-S.; Huffman, J. C.; Christou, G. *Inorg. Chem.* **1995**, *34*, 4167. (k) Salah El Fallah, M.; Rentschler, E.; Caneschi, A.; Gatteschi, D. *Inorg. Chim. Acta* **1996**, *247*, 231. (l) Escuer, A.; Font-Bardia, M.; Kumar, S. B.; Solans, X.; Vicente, R. *Polyhedron* **1999**, *18*, 909.

(13) (a) Blake, A. J.; Brechin, E. K.; Codron, A.; Gould, R. O.; Grant, C. M.; Parsons, S.; Rawson, J. M.; Winpenny, R. E. P. *J. Chem. Soc., Chem. Commun.* **1995**, 1983. (b) Faus, J.; Lloret, F.; Julve, M.; Clemente-Juan, J. M.; Munoz, M. C.; Solans, X.; Font-Bardia, M. *Angew. Chem.* **1996**, *108*, 1591. (c) Röder, J. C.; Meyer, F.; Pritzkow, H. *Chem. Commun.* **2001**, 2176. (d) Papaefstathiou, G. S.; Escuer, A.; Vicente, R.; Font-Bardia, M.; Solans, X.; Perlepes, S. P. *Chem. Commun.* **2001**, 2414. (e) Murie, M.; Stoeckli-Evans, H.; Güdel, H. U. *Angew. Chem., Int. Ed.* **2001**, *40*, 1957. (f) Andres, H.; Basler, R.; Blake, A. J.; Cadiou, C.; Chaboussant, G.; Grant, C. M.; Güdel, H.-U.; Murrie, M.; Parsons, S.; Paulsen, C.; Semandini, F.; Villar, V.; Wernsdorfer, W.; Winpenny, R. E. P. *Chem.—Eur. J.* **2002**, *8*, 4867. (g) Adams, H.; Clunas, S.; Fenton, D. E.; Towers, D. N. *J. Chem. Soc., Dalton Trans.* **2002**, 3933. (h) Dell'Amico, D. B.; Bradicich, C.; Calderazzo, F.; Guardini, A.; Labella, L.; Marchetti, F.; Tomei, A. *Inorg. Chem.* **2002**, *41*, 2814. (i) Diamantopoulou, E.; Rabtopoulou, C. P.; Terzis, A.; Tangoulis, V.; Perlepes, S. P. *Polyhedron* **2002**, *21*, 2117. (j) Gaynor, D.; Starikova, Z. A.; Ostrovsky, S.; Haase, W.; Nolan, K. B. *Chem. Commun.* **2002**, 506. (k) Aromi, G.; Bell, A. R.; Helliwell, M.; Raftery, J.; Teat, S. J.; Timco, G. A.; Roubeau, O.; Winpenny, R. E. P. *Chem.—Eur. J.* **2003**, *9*, 3024. (l) Lin, X.; Doble, D. M. J.; Blake, A. J.; Harrison, A.; Wilson, C.; Schröder, M. *J. Am. Chem. Soc.* **2003**, *125*, 9476. (m) Liu, Y.; Kravtsov, V.; Walsh, R. D.; Poddar, P.; Srikanth, H.; Eddaoudi, M. *Chem. Commun.* **2004**, 2806. (n) Keene, T. D.; Hursthouse, M. B.; Price, D. J. *New J. Chem.* **2004**, *28*, 558. (o) Wei, Y.; Hou, H.; Fan, Y.; Zhu, Y. *Eur. J. Inorg. Chem.* **2004**, 3946. (p) Pardo, E.; Morales-Osorio, I.; Julve, M.; Lloret, F.; Cano, J.; Ruiz-Gareia, R.; Pasán, J.; Ruis-Pérez, C.; Ottenwaelder, X.; Journaux, Y. *Inorg. Chem.* **2004**, *43*, 7594. (q) Wörl, S.; Pritzkow, H.; Fritsky, I. O.; Krämer, R. *Dalton Trans.* **2005**, 27. (r) Aromi, G.; Parsons, S.; Wernsdorfer, W.; Brechin, E. K.; McInnes, E. J. L. *Chem. Commun.* **2005**, 5038. (s) Bell, A.; Aromi, G.; Teat, S. J.; Wernsdorfer, W.; Winpenny, R. E. P. *Chem. Commun.* **2005**, 2808. (t) Abrahams, B. F.; Hudson, T. A.; Robson, R. *Chem.—Eur. J.* **2006**, *12*, 7095. (u) Luo, F.; Zheng, J.-M.; Kurmoo, M. *Inorg. Chem.* **2007**, *46*, 8448. (v) Papatriantafyllopoulou, C.; Aromi, G.; Tasiopoulos, A. J.; Nastopoulos, V.; Rabtopoulou, C.; Teat, S. J.; Escuer, A.; Perlepes, S. P. *Eur. J. Inorg. Chem.* **2007**, 2761. (w) Breeze, B. A.; Shanmugam, M.; Tuna, F.; Winpenny, R. E. P. *Chem. Commun.* **2007**, 5185.

(14) (a) Jiang, Y.-B.; Kou, H.-Z.; Wang, R.-J.; Cui, A. L.; Ribas, J. *Inorg. Chem.* **2005**, *44*, 709. (b) Stamatotos, T. C.; Abboud, K. A.; Perlepes, S. P.; Christou, G. *Dalton Trans.* **2007**, 3861. (c) Papatriantafyllopoulou, C.; Jones, L. F.; Nguen, T. D.; Matamoros-Salvador, N.; Cunha-Silva, L.; Paz, F. A. A.; Rocha, J.; Evangelisti, M.; Brechin, E. K.; Perlepes, S. P. *Dalton Trans.* **2008**, 3153. (d) Stamatatos, T. C.; Escuer, A.; Abboud, K. A.; Raptopoulou, C. P.; Perlepes, S. P.; Christou, G. *Inorg. Chem.* **2008**, *47*, 11825.

(15) Khanra, S.; Weyhermüller, T.; Rentschler, E.; Chaudhuri, P. *Inorg. Chem.* **2005**, *44*, 8176.

(16) Miyasaka, H.; Saitoh, A.; Yanagida, S.; Kachi-Terajima, C.; Sugiura, K.; Yamashita, M. *Inorg. Chim. Acta* **2005**, *358*, 3525.

(17) Chaudhuri, P.; Weyhermüller, T.; Wagner, R.; Khanra, S.; Biswas, B.; Bothe, E.; Bill, E. *Inorg. Chem.* **2007**, *46*, 9003.

(18) (a) Ross, S.; Weyhermüller, T.; Bill, E.; Bothe, E.; Flörke, U.; Wieghardt, K.; Chaudhuri, P. *Eur. J. Inorg. Chem.* **2004**, 984. (b) Ross, S.; Weyhermüller, T.; Bill, E.; Wieghardt, K.; Chaudhuri, P. *Inorg. Chem.* **2001**, *40*, 6656. (c) Chaudhuri, P.; Winter, M.; Flörke, U.; Haupt, H.-J. *Inorg. Chim. Acta* **1995**, *232*, 125. (d) Weyhermüller, T.; Wagner, R.; Khanra, S.; Chaudhuri, P. *Dalton Trans.* **2005**, 2539.

(19) (a) Milios, C. J.; Stamatatos, T. C.; Perlepes, S. P. *Polyhedron* **2006**, *25*, 134. (b) Stamatatos, T. C.; Diamantopoulou, E.; Taziopoulos, A.; Psycharis, V.; Vicente, R.; Raptopoulou, C. P.; Nastopoulos, V.; Escuer, A.; Perlepes, S. P. *Inorg. Chim. Acta* **2006**, *359*, 4149. (c) Miyasaka, H.; Furukawa, S.; Yanagida, S.; Suguira, K.; Yamashita, M. *Inorg. Chim. Acta* **2004**, *357*, 1619.

Scheme 1

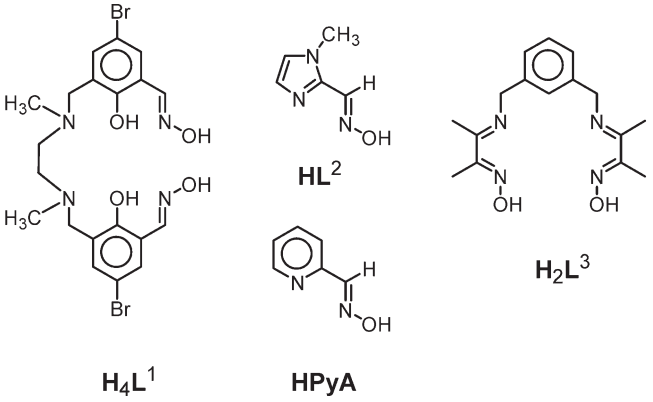

each other and a nonanuclear Ni(II) complex with PyA^- has been reported previously by us,[15] we have included the nonanuclear Ni(II) complex with $[L^2]^-$, complex **2**, in this paper for the sake of comparison. As earlier,[17] we will show a stronger σ-donor ability of the pyridine-N than that of the imidazole-N.

Experimental Section

Materials and Physical Measurements. Reagent- or analytical-grade materials were obtained from commercial suppliers and used without further purification. Elemental analyses (C, H, N, and Ni) were performed by the Microanalytical Laboratory, Mülheim, Germany. Fourier-transform IR spectra of the samples in KBr disks were recorded with a Perkin-Elmer 2000 FT-IR instrument. Magnetic susceptibilities of powdered samples were recorded with a SQUID magnetometer in the temperature range 2−290 K with an applied field of 1 T. Experimental susceptibility data were corrected for the underlying diamagnetism using Pascal's constants and for the temperature-independent paramagnetism contributions (100×10^{-6} cm^3 mol^{-1}).[5] Mass spectra were recorded with either a Finnigan MAT 8200 (electron ionization) or a MAT95 (electrospray ionization, ESI-MS) instrument. A Bruker DRX 400 instrument was used for NMR spectroscopy.

Preparations. The ligands HPyA and HL^2 were prepared as described previously.[17,18] Ligand H_2L^3 was isolated with a good yield (∼80%) by the condensation of *m*-xylenediamine and diacetylmonoxime in a 1:2 molar ratio by using the same protocol as described before.[17]

The compartmental dioxime ligand H_4L^1 was obtained as the dihydrochloride by the condensation of the dialdehyde, N,N′-dimethyl-N,N′-ethylenebis(5-bromo-3-formyl-2-hydroxybenzylamine), with hydroxylamine. To a suspension of the dialdehyde (7.07 g, 13.75 mmol) in methanol (120 mL) was added a solution of hydroxylamine hydrochloride (2.41 g, 35 mmol) in water (15 mL), yielding a clear light-brown solution. The solution was refluxed for 1 h to form a white-cream powder, which was separated by filtration, washed with methanol, and air-dried. Yield: 8.25 g of $H_4L^1 \cdot 2HCl$ (∼97%). M.P. 208−209° (dec.). EI-MS (*m*/*z*): 527 (0.77%) [$C_{20}H_{24}Br_2O_4N_4$−OH], 271 (34.6%) [$C_{10}H_{13}BrO_2N_2$]. ^{1}H NMR (400 MHz, in CD_3OD): δ 8.28 (s, 2H; CH=N), 7.67−7.64 (m, 4H, ring proton), 4.44 (s, 4H, Ar−CH_2−N), 3.72 (s, 4H, −CH_2), 2.88 (s, 6H, N−CH_3). Selected IR data of $H_4L^1 \cdot 2HCl$ (KBr, cm^{-1}): 3540, 3468, 3211, 3080, 2968, 2559, 1623, 1600, 1473, 1445, 1430, 1298, 1259, 1041, 1011, 997, 965, 952, 878, 781, 685, 628.

The starting dialdehyde was obtained as described in the literature[20] by refluxing a solution of N,N′-dimethylethylenediamine (50 mmol), 5-bromosalicylaldehyde (100 mmol), and paraformaldehyde (134 mmol) in distilled ethanol (300 mL) for 5 days. Yield: 7.1 g (∼ 26%). EI-MS (*m*/*z*): 514 $[M]^+$, 256 $[M/2]^+$ (100%).

$[Ni_4(HL^1)_2(\mu\text{-}OAc)_2(MeOH)] \cdot 2.5MeOH$ ($1 \cdot 2.5MeOH$). To a light-green solution of $Ni(OAc)_2 \cdot 4H_2O$ (0.60 g; 2.5 mmol) in methanol (25 mL) was added solid H_4L^1 (0.62 g; 1 mmol) with stirring, followed by the addition of Et_3N (0.26 mL, 2 mmol) and NaOAc (0.16 g; 2 mmol), and the resulting solution was stirred for 1 h. Slow evaporation of the solvent resulted in the precipitation of a light-green microcrystalline solid. X-ray-quality crystals were obtained by slow evaporation of a methanol solution. Yield: 135 mg. Anal. calcd for $C_{47.5}H_{62}Br_4N_8Ni_4O_{15.5}$: C, 36.87; H, 4.04; N, 7.24; Ni, 15.17. Found: C, 36.6; H, 3.8; N, 7.3; Ni, 15.3. IR (KBr, cm^{-1}): 3448, 2963, 1636, 1567, 1449, 1292, 1036, 834, 691.

$[Ni_9(L^2)_{10}(\mu_3\text{-}OH)_2(\mu\text{-}OH)_2(\mu\text{-}OH_2)_2(H_2O)_6](ClO_4)_4 \cdot 8MeCN \cdot H_2O$ ($2 \cdot 8MeCN \cdot H_2O$). The pH of an aqueous solution (25 mL) of $NiCl_2 \cdot 6H_2O$ (0.47 g; 2 mmol) and HL^2 (0.25 g; 2 mmol) was adjusted with dilute NaOH to a pH of ∼8.0, to which $NaClO_4$ (0.36 g; 3 mmol) was added to provide counteranions. The light-brown−orange solution was filtered and allowed to slowly concentrate at room temperature to isolate a light-orange microcrystalline solid. X-ray-quality crystals were obtained by slow evaporation of a CH_3CN-H_2O (4:1) solution of the light-orange solid. The crystals were collected by filtration and air-dried. Yield: 600 mg (∼80%). Anal. calcd for $C_{66}H_{106}N_{38}O_{23}(ClO_4)_4$: C, 29.08; H, 3.92; N, 19.53; Ni, 19.38. Found: C, 28.9; H, 3.8; N, 19.8; Ni, 19.7. IR (KBr, cm^{-1}): 1634, 1564, 1457, 1291, 1089, 1037, 963, 862, 626, 519.

$[Ni_6(L^2)_9(HL^2)(MeOH)(H_2O)_2](ClO_4)_3 \cdot 2H_2O$ ($3 \cdot 2H_2O$). To a light-green solution of $Ni(ClO_4)_2 \cdot 6H_2O$ (0.37 g; 1 mmol) in methanol (25 mL) was added solid 1-methyl-2-imidazoleoxime (0.25 g; 2 mmol) with stirring, followed by the addition of Et_3N (0.26 mL; 2 mmol); the resulting solution was stirred for 30 min. The solution was allowed to concentrate slowly at room temperature to yield a light-orange microcrystalline solid. X-ray-quality crystals were obtained from a CH_3OH/CH_2Cl_2 (4:1) solution. Yield: 200 mg (35%). Anal. calcd for $Ni_6C_{51}H_{73}N_{30}O_{15}(ClO_4)_3$: C, 30.68; H, 3.69; N, 21.04; Ni, 17.63. Found: C, 30.8; H, 3.6; N, 21.3; Ni, 17.8. IR (KBr, cm^{-1}): 1633, 1560, 1384, 1289, 1087, 1037, 962, 860, 625.

$[Ni_6(L^3)_3(\mu_3\text{-}O)_2](ClO_4)_2 \cdot 3MeCN$ ($4 \cdot 3MeCN$). To a solution of $NiSO_4 \cdot 6H_2O$ (0.52 g; 2 mmol) in methanol (25 mL) was added the ligand dioxime H_2L^3 (0.30 g; 1 mmol) with stirring, followed by the addition of NaOAc (0.24 g; 3 mmol). The resulting brown solution was refluxed for 0.5 h, and then $NaClO_4$ (0.5 g) was added to procure a brown microcrystalline solid, which was separated by filtration. Yield: 250 mg (50%). X-ray-quality crystals were obtained from a methanol solution. Anal. calcd for $C_{54}H_{69}N_{15}O_8Ni_6(ClO_4)_2$: C, 40.35; H, 4.33; N, 13.07; Ni, 21.91. Found: C, 40.0; H, 4.2; N, 12.9; Ni, 21.8. IR (KBr, cm^{-1}): 1636, 1560, 1384, 1246, 1100, 1037, 699, 625. MS (ESI pos in DMF-CH_3CN) (*m*/*z*): 1382 $[M-ClO_4]^+$, 642.1 $[(M-2ClO_4)/2]$ (100%). MS (ESI neg in DMF-CH_3CN) (*m*/*z*): 99.1 (100%) $[ClO_4]$.

X-Ray Crystallographic Data Collection and Refinement of the Structures. Single crystals of $1 \cdot 2.5MeOH$, $2 \cdot 8MeCN \cdot H_2O$, $3 \cdot 2H_2O$, and $4 \cdot 3MeCN$ were coated with perfluoropolyether, picked up with nylon loops, and immediately mounted in the nitrogen cold stream of a Bruker-Nonius CCD diffractometer, equipped with a Mo-target rotating-anode X-ray source. Graphite monochromated Mo Kα radiation ($\lambda = 0.71073$ Å) was used. Final cell constants were obtained from least-squares fits of several thousand strong reflections. Intensity data were corrected for absorption using redundant reflection intensities with the program SADABS.[21] Structures were readily solved by Patterson methods and subsequent difference Fourier techniques. The Siemens ShelXTL[22] software package was used

(20) Yonemura, M.; Matsumura, Y.; Furutachi, H.; Ohba, M.; Okawa, H. *Inorg. Chem.* **1997**, *36*, 2711.

(21) *SADABS*, version 2006/1; Bruker AXS Inc.: Madison, WI, 2006.

(22) *ShelXTL 6.14*; Bruker AXS Inc.: Madison, WI, 2003.

Table 1. Crystallographic Data for $1\cdot 2.5CH_3OH$, $2\cdot 8CH_3CN\cdot H_2O$, $3\cdot 2H_2O$, and $4\cdot 3CH_3CN$

	$1\cdot 2.5CH_3OH$	$2\cdot 8CH_3CN\cdot H_2O$	$3\cdot 2H_2O$	$4\cdot 3CH_3CN$
chem. formula	$C_{47.5}H_{62}Br_4N_8Ni_4O_{15.5}$	$C_{66}H_{106}Cl_4N_{38}Ni_9O_{39}$	$C_{51}H_{73}Cl_3N_{30}Ni_6O_{27}$	$C_{54}H_{69}Cl_2N_{15}Ni_6O_{16}$
crystal size, mm^3	$0.10 \times 0.02 \times 0.02$	$0.09 \times 0.08 \times 0.07$	$0.15 \times 0.11 \times 0.05$	$0.10 \times 0.03 \times 0.03$
fw	1291.05	2726.08	1997.00	1607.40
space group	$P\bar{1}$, No. 2	$P\bar{1}$, No. 2	$P\bar{1}$, No. 2	$C2/c$, No. 15
a, Å	11.7718(11)	16.7841(6)	13.9793(7)	18.8266(11)
b, Å	14.5405(15)	16.9192(6)	15.2739(8)	22.1141(13)
c, Å	18.589(2)	23.7893(9)	20.9404(13)	15.5820(9)
α, deg	72.583(6)	106.789(3)	90.848(3)	90
β, deg	79.072(8)	91.733(3)	92.412(3)	92.298(5)
γ, deg	69.254(8)	110.043(3)	94.460(3)	90
V, Å	2826.6(5)	6012.8(4)	4452.9(4)	6482.1(7)
Z	2	2	2	4
T, K	100(2)	100(2)	100(2)	100(2)
ρ calcd, g cm^{-3}	1.818	1.201	1.489	1.647
refl. collected/$2\theta_{max}$	19476/52.00	137520/65.00	44220/45.00	42602/55.00
unique reflns/$I > 2\sigma(I)$	10343/8096	43102/33607	11392/8658	7437/5743
no. of params/restraints	743/4	1515/262	1041/32	434/0
λ, Å/μ(Kα), cm^{-1}	0.71073/42.12	0.71073/15.06	0.71073/14.17	0.71073/18.67
R1[a]/goodness of fit[b]	0.0358/1.036	0.0440/1.044	0.0922/1.128	0.0412/1.038
wR2[c] ($I > 2\sigma(I)$)	0.0618	0.1253	0.1991	0.0770
residual density, e $Å^{-3}$	+0.63/−0.58	+1.98/−1.45	+1.28/−0.91	+0.44/−1.03

[a] Observation criterion: $I > 2\sigma(I)$. $R1 = \sum ||F_o| - |F_c|| / \sum |F_o|$. [b] $GoF = [\sum w(F_o^2 - F_c^2)^2]/(n-p)]^{1/2}$. [c] $wR2 = [\sum w(F_o^2 - F_c^2)^2] / \sum [w(F_o^2)^2]]^{1/2}$ where $w = 1/\sigma^2(F_o^2) + (aP)^2 + bP$, $P = (F_o^2 + 2F_c^2)/3$.

for solution and artwork of the structures; ShelXL97[23] was used for the refinement. All non-hydrogen atoms were anisotropically refined except for some disordered fragments. Details are given below. Hydrogen atoms bound to carbon and nitrogen were placed at calculated positions and refined as riding atoms with isotropic displacement parameters. Hydrogen atoms bound to oxygen atoms were, where appropriate, located from the difference map and refined with restrained bond distances. Crystallographic data of the compounds are listed in Table 1.

A methanol molecule in $1\cdot 2.5$MeOH located next to a center of inversion (O110 and C111) was found to be disordered over two sites. An occupation factor of 0.5 was therefore used for the refinement. DFIX was used to constrain the O−C distance. Hydrogen atom distances of H1, H66, and H100 were restrained to be equal within errors using the SADI instruction of ShelXL97 (four restraints). $2\cdot 8MeCN\cdot H_2O$ represents the crystallographically refined composition of **2**, but at least three more acetonitrile molecules were found to be extremely disordered. Several attempts to refine a disorder model were not satisfying. The program Platon-Squeeze[24] was therefore used to remove the diffuse density from a volume of about 380 $Å^3$/asymmetric unit, which represents about 12.6% of the total volume. Perchlorate anions containing Cl3 and Cl4 were split on two positions and were refined with restrained distances and thermal displacement parameters using SAME and EADP instructions. DFIX was used to constrain the geometry of two acetonitrile molecules (N550−C552, N620−C622). A total of 262 restraints were used.

Two perchlorate anions in $3\cdot 2H_2O$ containing C170 and C180 were refined with restrained bond distances using SADI. The oxygen atoms at C170 were only isotropically refined since they show extreme disorder. A split atom model was tried but not successful. Hydrogen atoms at O400, O410, O420, and O430 could not be reliably located from the difference map. A total of 32 restraints were used.

The central μ_3-oxo group in $4\cdot 3$MeCN was found to be disordered. Two positions with equal thermal displacement parameters and with almost equal occupation were refined.

(23) Sheldrick, G. M. *ShelXL97*; University of Göttingen: Göttingen, Germany, 1997.

(24) Platon Program Suite: Spek, A. L. *J. Appl. Crystallogr.* **2003**, *36*, 7.

Results and Discussion

The new dioxime ligand H_4L^1 provides two dissimilar N_2O_2 metal-binding sites but with a common phenolate bridging group. The polynucleating nature of the ligand H_4L^1 prompted us to use arbitrarily a ratio of Ni/L^1 (2.5:1) in which nickel was in excess with an expectation for isolation of a polynickel complex. The synthetic method results in isolation of an unusual tetranickel(II) compound, **1**, containing a Ni/L^1 ratio of 2:1, which can be considered as a dimer of a dimer bridged through an oxime oxygen; such a bridging mode of oxime functionality is unprecedented, thus fulfilling our expectation from a new ligand. It is interesting to note that the ESI-MS (positive + negative) spectrum of **1** in methanol exhibits peaks at m/z 776.9, 1486.1, and 2176.5 corresponding to Ni_3L^1, $Ni_4(L^1)_2$, and $Ni_7(L^1)_3$ species, respectively, thus indicating the possibility of isolating other species also. In contrast, the spectrum of **1** in DMF-MeOH in the positive ion mode of ESI-MS yields predominantly the dimeric species Ni_2HL^1 (m/z 655.9, 100%) and also indicates the presence of one OAc− and the coordinated methanol-depleted species [$(Ni_4(HL^1)_2OAc$, m/z 1369, ∼10%)].

Considering the similar ligation properties[16,17] of HL^2 and pyridine-2-aldoxime, we performed a reaction of Ni(II) ions with HL^2 in aqueous solution under the conditions which yielded a nonanuclear Ni(II) complex with pyridine-2-aldoxime, as reported earlier by us. It was gratifying to isolate the expected Ni_9 species, **2**, with the ligand HL^2. Interestingly, in methanolic solution, in contrast, a hexanuclear Ni(II) complex, **3**, could be isolated. All of our attempts to improve the yield of **3** by changing the ratio L^2/Ni failed.

Because the relevant bands in the IR spectra of related compounds containing oxime ligands have been reported previously by us[8,18] and others,[19] we refrain from discussing them for **1**−**4** again. The bands are given in the Experimental Section.

ESI-MS in both the positive and the negative ion mode has been proven to be a very useful analytical tool for characterizing complex **4**, which shows the species $[M-2ClO_4]$ as the

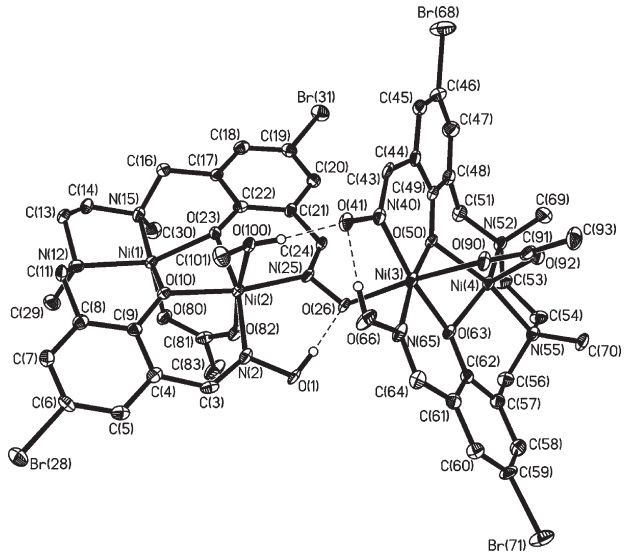

Figure 1. ORTEP diagram of complex **1**, Ni^{II}_4, with 40% probability of the ellipsoids.

base peak (100%) in the positive mode. As expected, the negative ion mode exhibits the perchlorate ion as the base peak.

Description of the Structures

$[Ni_4(HL^1)_2(\mu\text{-}OAc)_2(MeOH)]\cdot 2.5MeOH$ (Complex $1\cdot 2.5MeOH$). The structure of this compound consists of a discrete neutral tetranuclear unit $[Ni_4(HL^1)_2(\mu\text{-}OAc)_2(MeOH)]$. Only one MeOH molecule is coordinated to a nickel center, Ni(2). An ORTEP plot with the atom labeling scheme is presented in Figure 1. Table 2 summarizes selected bond lengths and angles. Two of the oxygens belonging to the oxime NO groups are protonated, O(1) and O(66), and as expected strongly are hydrogen-bonded to nearby oxime oxygens O(26) and O(41) with O···O bond distances of 2.551 and 2.591 Å, respectively. The coordinated methanol is also hydrogen-bonded to O(41) with an O(41)···O(100) separation of 2.718 Å. These H atoms have been detected as peaks assignable to protons in the later refinement stages; they were included in these positions in the final refinement cycle. Relevant hydrogen-bonded distances are included as Supporting Information in Table S1. The presence of the protons attached to O(1) and O(66) renders each ligand trianionic, and thus, each ligand supplies three negative charges, $[HL^1]^{3-}$, to the charge-balance considerations. A significant amount of hydrogen bonding is also prevalent with solvent molecules, with the O···O separations lying in the range 2.738−2.888 Å.

Tetranuclear complex **1** can be considered as consisting of two dinuclear Ni(II) entities, Ni(1)/Ni(2) and Ni(3)/Ni(4), which are held together by a single deprotonated oxime oxygen O(26); such a single bridging oximate is unprecedented in the literature. As expected, the Ni centers bridged by a single oxime group are separated by a comparatively long distance at Ni(2)N(25)O(26)Ni(3) ∼4.712 Å. Each dinuclear center is comprised of a five-coordinated Ni(1) or Ni(4) with distorted square pyramidal N_2O_3 environments and a distorted octahedral nickel(II) center, Ni(2) or Ni(3), with N_2O_4 donor atoms. Within the dinuclear units, the five-coordinate nickel

Table 2. Selected Bond Lengths [Å] and Angles [deg] for Complex $1\cdot 2.5CH_3OH$

Ni(1)−O(80)	1.970(2)
Ni(1)−O(23)	1.980(2)
Ni(1)−O(10)	2.002(2)
Ni(1)−N(12)	2.056(3)
Ni(1)−N(15)	2.086(3)
Ni(1)−Ni(2)	2.9204(7)
Ni(2)−N(25)	1.986(3)
Ni(2)−O(10)	1.998(2)
Ni(2)−O(23)	2.018(2)
Ni(2)−N(2)	2.020(3)
Ni(2)−O(82)	2.103(2)
Ni(2)−O(100)	2.133(2)
Ni(3)−O(50)	2.002(2)
Ni(3)−N(65)	2.008(3)
Ni(3)−N(40)	2.014(3)
Ni(3)−O(63)	2.020(2)
Ni(3)−O(26)	2.082(2)
Ni(3)−O(90)	2.140(2)
Ni(3)−Ni(4)	2.9498(7)
Ni(4)−O(92)	1.967(2)
Ni(4)−O(63)	1.991(2)
Ni(4)−O(50)	2.004(2)
Ni(4)−N(52)	2.058(3)
Ni(4)−N(55)	2.079(3)
O(1)−N(2)	1.381(4)
N(2)−C(3)	1.283(4)
C(24)−N(25)	1.282(4)
N(25)−O(26)	1.378(3)
N(40)−C(43)	1.281(4)
N(40)−O(41)	1.374(4)
C(64)−N(65)	1.282(4)
N(65)−O(66)	1.398(4)
O(80)−Ni(1)−O(23)	106.41(10)
O(80)−Ni(1)−O(10)	99.11(10)
O(23)−Ni(1)−O(10)	79.27(9)
O(80)−Ni(1)−N(12)	102.62(11)
O(23)−Ni(1)−N(12)	150.64(11)
O(10)−Ni(1)−N(12)	92.06(11)
O(80)−Ni(1)−N(15)	97.08(11)
O(23)−Ni(1)−N(15)	92.94(10)
O(10)−Ni(1)−N(15)	163.46(11)
N(12)−Ni(1)−N(15)	87.68(11)
O(80)−Ni(1)−Ni(2)	87.54(7)
O(23)−Ni(1)−Ni(2)	43.58(6)
O(10)−Ni(1)−Ni(2)	43.07(7)
N(12)−Ni(1)−Ni(2)	135.12(8)
N(15)−Ni(1)−Ni(2)	134.92(8)
N(25)−Ni(2)−O(10)	169.32(10)
N(25)−Ni(2)−O(23)	91.11(10)
O(10)−Ni(2)−O(23)	78.48(9)
N(25)−Ni(2)−N(2)	101.30(12)
O(10)−Ni(2)−N(2)	89.28(11)
O(23)−Ni(2)−N(2)	166.81(11)
N(25)−Ni(2)−O(82)	88.44(10)
O(10)−Ni(2)−O(82)	93.76(9)
O(23)−Ni(2)−O(82)	89.31(9)
N(2)−Ni(2)−O(82)	86.59(11)
N(25)−Ni(2)−O(100)	86.81(10)
O(10)−Ni(2)−O(100)	91.29(9)
O(23)−Ni(2)−O(100)	92.86(9)
N(2)−Ni(2)−O(100)	92.30(10)
O(82)−Ni(2)−O(100)	174.81(9)
N(25)−Ni(2)−Ni(1)	128.42(8)
O(10)−Ni(2)−Ni(1)	43.17(7)
O(23)−Ni(2)−Ni(1)	42.58(6)
N(2)−Ni(2)−Ni(1)	124.29(8)
O(82)−Ni(2)−Ni(1)	73.12(6)
O(100)−Ni(2)−Ni(1)	111.56(7)
O(50)−Ni(3)−N(65)	169.29(10)
O(50)−Ni(3)−N(40)	89.92(11)
N(65)−Ni(3)−N(40)	100.59(12)
O(50)−Ni(3)−O(63)	79.57(9)
N(65)−Ni(3)−O(63)	89.83(11)
N(40)−Ni(3)−O(63)	169.17(11)
O(50)−Ni(3)−O(26)	96.38(9)
N(65)−Ni(3)−O(26)	85.29(11)

Table 2. Continued

N(40)−Ni(3)−O(26)	92.59(10)
O(63)−Ni(3)−O(26)	91.17(9)
O(50)−Ni(3)−O(90)	90.63(10)
N(65)−Ni(3)−O(90)	87.37(11)
N(40)−Ni(3)−O(90)	89.84(10)
O(63)−Ni(3)−O(90)	87.70(9)
O(26)−Ni(3)−O(90)	172.58(10)
O(50)−Ni(3)−Ni(4)	42.61(6)
N(65)−Ni(3)−Ni(4)	127.03(8)
N(40)−Ni(3)−Ni(4)	127.03(9)
O(63)−Ni(3)−Ni(4)	42.29(7)
O(26)−Ni(3)−Ni(4)	111.07(7)
O(90)−Ni(3)−Ni(4)	72.71(7)
O(92)−Ni(4)−O(63)	104.23(10)
O(92)−Ni(4)−O(50)	97.26(10)
O(63)−Ni(4)−O(50)	80.19(9)
O(92)−Ni(4)−N(52)	102.88(11)
O(63)−Ni(4)−N(52)	152.47(11)
O(50)−Ni(4)−N(52)	91.73(10)
O(92)−Ni(4)−N(55)	97.66(11)
O(63)−Ni(4)−N(55)	95.22(10)
O(50)−Ni(4)−N(55)	165.06(10)
N(52)−Ni(4)N(55)	85.85(11)
O(92)−Ni(4)−Ni(3)	87.72(7)
O(63)−Ni(4)−Ni(3)	43.03(6)
O(50)−Ni(4)−Ni(3)	42.55(7)
N(52)−Ni(4)−Ni(3)	134.25(8)
N(55)−Ni(4)−Ni(3)	137.36(8)

atom is bridged to the six-coordinate nickel through an acetate group. Additionally, the dinuclear N(II) centers are doubly bridged by phenoxide oxygens, O(50) and O(63) for the Ni(4)/Ni(3) center but O(23) and O(10) for the Ni(2)/Ni(1) center, with the Ni−O−Ni angles lying in the narrow range of 93.8(1)−94.8(1)°. The phenoxide-bridging networks Ni_2O_2 comprising the equatorial planes of the nickel centers are not completely planar, with the atoms deviating from the mean planes by 0.25 Å for the Ni(1)/Ni(2) and 0.22 Å for the Ni(3)/Ni(4) dinuclear centers. The distances between the metal centers are Ni(1)···Ni(2) at 2.920(1) and Ni(3)···Ni(4) at 2.950(1) Å. The deviations of the five-coordinated nickel centers from the mean planes comprising Ni(1)N(15)N-(12)O(10)O823) and Ni(4)N(55)N(52)O(50)O(63) are 0.395 and 0.370 Å, respectively. The Ni−N(amine) bond length with an average of 2.070 ± 0.015 Å is slightly longer than the Ni−N(oxime) lengths at an average of 2.007 ± 0.02 Å, as expected. The Ni−O(phenoxide) (average 2.002 ± 0.02 Å) and Ni−O(acetate) (average 2.045 ± 0.08 Å) bond distances are very similar to those of the analogous complexes reported previously by us[8,17,25] and others.[26] The N−O and C═N bond lengths and C−N−O bond angles of the oxime groups are found to be very similar to those of other comparable structures. That the bridging Ni(3)−O(26)−N(25)−Ni(2) is not planar is shown by the dihedral angle θ of 47.2° between the planes comprising Ni(3)O(26)N(25) and Ni(2)N(25)O(26). It is interesting to note that a similar dihedral angle has been obtained previously for compound $[LNi^{II}Ni^{II}(PyA-Ph)_3]^+$, although with three bridging oximate groups.[17]

$[Ni_9(L^2)_{10}(\mu_3\text{-}OH)_2(\mu\text{-}OH)_2(\mu_2\text{-}OH_2)_2(OH_2)_6](ClO_4)_4\cdot 8MeCN\cdot H_2O$ (Complex $2\cdot 8MeCN\cdot H_2O$). The molecular

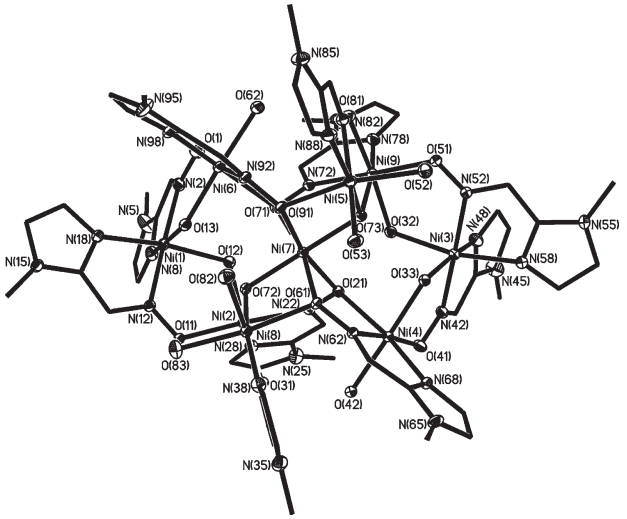

Figure 2. Molecular structure of the cation in complex 2, Ni^{II}_9.

structure of complex **2** consists of an enneanuclear tetracation, four perchlorate anions, and solvate molecules. A view of the cation in **2** is shown in Figure 2. This compound joins a small family of structurally characterized enneanuclear Ni(II) clusters with only N- and O-donor ligands.[15,19b] There are two different coordination modes of the oximate groups: (i) ubiquitous two-atom N−O bridging groups, N(2)−O(1), N(12)−O(11), N(32)−O(31), N(42)−O(41), N(52)−O(51), and N(82)−O(81), and (ii) μ_2-O bridging oximates, O(21), O(61), O(71), and O(91); these two different types of bridging oximic groups in the same compound are extremely rare.[7,19a] The cation in **2** can be described as two $[Ni_4(L^2)_5(\mu_3\text{-}OH)(\mu_2\text{-}OH)(\mu_2\text{-}OH_2)(H_2O)_3]^+$ subunits connected to a centrally placed Ni(II) ion, Ni(7), through four μ_2-oximate oxygens Ni−O(N)−Ni, that is, O(21), O(61), O(71), and O(91), and two trans-disposed μ_3-OH groups, O(72) and O(73), thus yielding an octahedral $Ni(7)O_6$ core (Figure 2). The nickel centers are six-coordinated and can be divided on the basis of the donor atoms into three categories: (a) one center with six oxygen ligands, $Ni(7)O_6$, (b) two centers, Ni(1) and Ni(3), with N_4O_2 donor sets (two imidazole nitrogens, two oximic nitrogens, and two μ_2-OH bridging oxygens), and (c) six centers, Ni(2), Ni(4), Ni(5), Ni(6), Ni(8), and Ni(9), with N_2O_4 donor atoms, out of which the Ni(5) and Ni(8) atoms are each coordinated to two terminal water molecules instead of one μ_2-OH_2 bridging oxygen for the other remaining four centers. The structure is identical with that described earlier with the $[PyA]^-$ monoanion (Scheme 1) by us[15] and later by others,[19b] and hence we are refraining from describing it again in detail. There are several moderately strong hydrogen bondings lying in a small range of 2.67−2.75 Å prevailing primarily between the oximate, hydroxo, and water oxygens. The hydrogen bonds involving the solvent molecules are, as expected, weaker (~2.9 Å) and not shown in Figure 2. Presumably, all of these hydrogen bonds are responsible for building up the supramolecular structure in **2**. All Ni−O and Ni−N bond lengths are in accord with a high-spin d^8 electron configuration description for the Ni centers with oximate ligands. A schematic Ni_9-core structure is shown in Figure 3. Table 3 summarizes selected bond lengths and angles for complex **2**.

$[Ni_6(L^2)_9(HL^2)(MeOH)(H_2O)_2](ClO_4)_3\cdot 2H_2O$ (Complex $3\cdot 2H_2O$). The structure of this compound consists of a

(25) Krebs, C.; Winter, M.; Weyhermüller, T.; Bill, E.; Wieghardt, K.; Chaudhuri, P. *J. Chem. Soc., Chem. Commun.* **1995**, 1913.

(26) See, for example: Nanda, K. K.; Das, R.; Thompson, L. K.; Venkatsubramanian, K.; Nag, K. *Inorg. Chem.* **1994**, *33*, 5934.

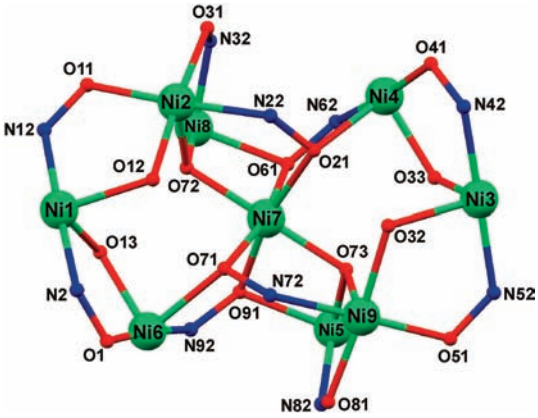

Figure 3. Metallic core in the Ni^{II}_9 complex (**2**).

discrete tricationic hexanuclear unit, $[Ni_6(L^2)_9(HL^2)(CH_3OH)(H_2O)_2]^{3+}$, whose molecular structure with the atom labeling scheme is presented in Figure 4. Table 4 lists selected bond lengths and angles for complex **3**. One of the oximic oxygens, O(11), is protonated. This H atom was detected as a peak assignable to a proton in the later refinement stages; it was included in the final refinement cycle. The presence of the proton attached to O(11) renders this ligand $[HL^2]$ neutral and thus, nine other ligands supply nine negative charges, $9[L^2]^-$, to the charge-balance considerations. Like complex **2**, two different coordination modes, (i) two-atom Ni−N−O−Ni bridging and (ii) monatomic O-bridging oximates, Ni−μ-O(N)−Ni, are found in the structure. Each nickel center is six-coordinated, but with different donor atoms, namely, NiN_6, NiO_6, NiN_3O_3, NiN_4O_2, and $NiNO_5$. The natures of the donor atoms are denoted below in detail for each center:

$Ni(1)(N_{Im})_2(N_{ox})_2(O_{ox})(OH_2)$,
$Ni(2)(N_{Im})_3(N_{ox})_3$,
$Ni(3)(O_{ox})_6$,
$Ni(4)(N_{Im})_2(N_{ox})(O_{ox})(OH_2)(OHCH_3)$,
$Ni(5)(N_{ox})(O_{ox})_5$, and
$Ni(6)(N_{Im})_3(N_{ox})_3$

where N_{Im}, N_{ox}, and O_{ox} represent imidazole-N, oximic-N, and oximic-O, respectively. As is seen, two water molecules are coordinated to the Ni(1) and Ni(4) centers, whereas a single methanol molecule is bound to the Ni(4) center. Noteworthy are the coordinated oximic oxygen atoms for Ni(3), of which four are of the μ-O type bridging two metal centers, Ni−O−Ni(3), while two are of a two-atom Ni−N−O−Ni(3) bridging mode. The Ni−N and Ni−O bond lengths are as expected for Ni(II) centers with oxime ligands and do not warrant any special discussion. There are hydrogen bondings, O(71)···O(11) at 2.539 and O(100)···O(51) at 2.729 Å, involving primarily the protonated oxime oxygen and water molecules.

$[Ni_6(L^3)_3(\mu_3\text{-}O)_2](ClO_4)_2\cdot 3MeCN$ (Complex $4\cdot 3MeCN$). The molecular structure of the dication in **4** can be viewed as two trinuclear $[Ni^{II}_3(\mu_3\text{-}O)]^{4+}$ units, in which each Ni(II) center is in distorted square-planar geometry with NiN_2O_2 cores. The deprotonated ligand $[L^3]^{2-}$ acts in a bis(bidentate) fashion to generate a hexanuclear complex, in which two oxo groups, O^{2-}, balance partially the positive charges due to divalent nickel centers. Each parent trinuclear unit is composed of three symmetry-independent

Table 3. Selected Bond Lengths [Å] and Angles [deg] for Complex $2\cdot 8CH_3CN\cdot H_2O$

Ni(1)−O(13)	2.0095(12)
Ni(1)−N(18)	2.0478(15)
Ni(1)−N(12)	2.0542(14)
Ni(1)−N(2)	2.0612(15)
Ni(1)−N(8)	2.0633(15)
Ni(1)−O(12)	2.1282(12)
Ni(2)−O(11)	2.0188(12)
Ni(2)−O(72)	2.0330(12)
Ni(2)−O(31)	2.0553(11)
Ni(2)−N(22)	2.0824(14)
Ni(2)−N(28)	2.0925(15)
Ni(2)−O(12)	2.1366(12)
Ni(3)−O(33)	2.0246(12)
Ni(3)−N(42)	2.0681(15)
Ni(3)−N(52)	2.0738(14)
Ni(3)−N(48)	2.0813(17)
Ni(3)−N(58)	2.0925(13)
Ni(3)−O(32)	2.1190(11)
Ni(4)−O(33)	2.0214(11)
Ni(4)−O(41)	2.0247(14)
Ni(4)−N(68)	2.0722(13)
Ni(4)−O(42)	2.0998(11)
Ni(4)−N(62)	2.1178(15)
Ni(4)−O(21)	2.1487(11)
Ni(5)−O(73)	2.0113(13)
Ni(5)−N(88)	2.0507(16)
Ni(5)−N(82)	2.0666(14)
Ni(5)−O(53)	2.0742(13)
Ni(5)−O(52)	2.1103(13)
Ni(5)−O(91)	2.1307(11)
Ni(6)−O(13)	1.9886(12)
Ni(6)−O(1)	2.0553(13)
Ni(6)−N(98)	2.0795(17)
Ni(6)−N(92)	2.1016(14)
Ni(6)−O(62)	2.1063(13)
Ni(6)−O(71)	2.1966(13)
Ni(7)−O(72)	1.9950(11)
Ni(7)−O(73)	2.0038(11)
Ni(7)−O(91)	2.1104(13)
Ni(7)−O(61)	2.1164(11)
Ni(7)−O(21)	2.1301(13)
Ni(7)−O(71)	2.1307(11)
Ni(8)−O(72)	2.0156(12)
Ni(8)−N(32)	2.0502(14)
Ni(8)−O(82)	2.0565(14)
Ni(8)−N(38)	2.0693(14)
Ni(8)−O(83)	2.0972(13)
Ni(8)−O(61)	2.1387(11)
Ni(9)−O(51)	2.0221(11)
Ni(9)−O(73)	2.0343(12)
Ni(9)−O(81)	2.0481(13)
Ni(9)−N(78)	2.0786(15)
Ni(9)−N(72)	2.0839(13)
Ni(9)−O(32)	2.1604(13)
N(12)−Ni(1)−N(2)	178.29(5)
O(13)−Ni(1)−N(8)	167.92(6)
N(18)−Ni(1)−O(12)	171.37(5)
O(11)−Ni(2)−N(22)	176.87(5)
O(72)−Ni(2)−N(28)	167.51(5)
O(31)−Ni(2)−O(12)	175.05(5)
N(42)−Ni(3)−N(52)	178.02(6)
O(33)−Ni(3)−N(48)	167.58(5)
N(58)−Ni(3)−O(32)	167.79(5)
O(33)−Ni(4)−O(42)	174.10(5)
O(41)−Ni(4)−N(62)	175.10(5)
N(68)−Ni(4)−O(21)	164.14(6)
O(73)−Ni(5)−N(88)	168.13(5)
N(82)−Ni(5)−O(53)	171.97(6)
O(52)−Ni(5)−O(91)	165.52(5)
O(1)−Ni(6)−N(92)	175.04(5)
O(13)−Ni(6)−O(62)	176.07(6)
N(98)−Ni(6)−O(71)	164.77(5)
O(72)−Ni(7)−O(73)	176.63(5)
O(91)−Ni(7)−O(21)	167.28(4)
O(61)−Ni(7)−O(71)	167.92(4)

Table 3. Continued

N(32)−Ni(8)−O(82)	175.28(6)
O(72)−Ni(8)−N(38)	168.30(6)
O(83)−Ni(8)−O(61)	171.20(5)
O(73)−Ni(9)−N(78)	169.09(5)
O(51)−Ni(9)−N(72)	178.09(6)
O(81)−Ni(9)−O(32)	174.81(4)
Ni(1)−O(12)−Ni(2)	108.44(5)
Ni(6)−O(13)−Ni(1)	115.45(6)
Ni(3)−O(32)−Ni(9)	110.54(5)
Ni(4)−O(33)−Ni(3)	114.42(6)
Ni(7)−O(72)−Ni(8)	102.62(4)
Ni(7)−O(72)−Ni(2)	113.65(6)
Ni(8)−O(72)−Ni(2)	112.63(5)
Ni(7)−O(73)−Ni(5)	102.10(6)
Ni(7)−O(73)−Ni(9)	113.60(5)
Ni(5)−O(73)−Ni(9)	112.40(5)
Ni(7)−O(71)−Ni(6)	112.59(6)
Ni(7)−O(61)−Ni(8)	94.73(4)
Ni(7)−O(91)−Ni(5)	94.82(5)
Ni(7)−O(21)−Ni(4)	114.60(5)
Ni(7)−O(21)−Ni(4)	114.60(5)
Ni(7)−O(61)−Ni(8)	94.73(4)

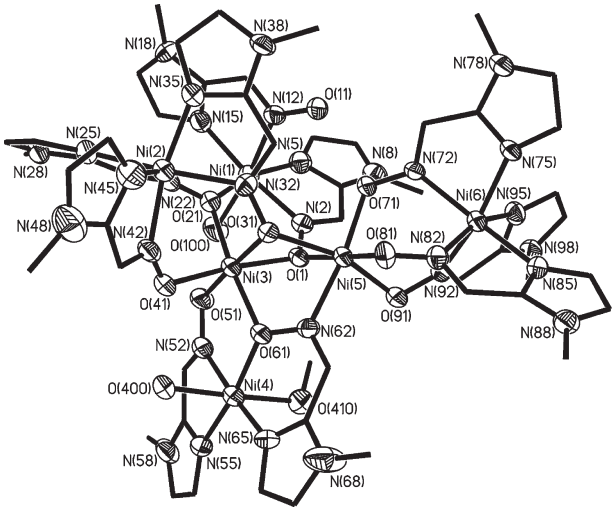

Figure 4. ORTEP diagram of complex **3**, Ni^{II}_6 with 50% probability of the ellipsoids. The C atoms are not labeled for the sake of clarity.

nickel(II) cations, each of which is four-coordinated, resulting in square-planar nickel(II) centers with the same chemical environments: one μ_3-oxide, one oximate-O, and two azomethine-N's as donor atoms.

The distances to the nickel atoms are within the observed ranges, Ni−N at ∼1.84 Å and Ni−O at ∼1.86 Å, for low-spin Ni(II) complexes and, together with the bond angles, are listed in Table 5. The trinuclear subunit thus formed is bonded to the other symmetry-related subunit through three deprotonated $[L^5]^{2-}$ ligands, which being bidentate are tied to three Ni(1)*, Ni(2)*, and Ni(3)* cations. The molecular structure of the hexanuclear dication in complex **4** is given in Figure 5. Although such μ_3-oxo bridging is ubiquitous for trivalent metal centers,[27] they are scarce for the divalent metal ions with a lower charge, as expected.[28]

(27) Cannon, R. D.; White, R. P. *Prog. Inorg. Chem.* **1988**, *36*, 195.

(28) (a) Humphrey, S. M.; Mole, R. A.; McPartlin, M.; McInnes, E. J. L.; Wood, P. T. *Inorg. Chem.* **2005**, *44*, 5981. (b) Singh, A.; Anandhi, U.; Cinellu, A.; Sharp, P. R. *Dalton Trans.* **2008**, 2314.

Table 4. Selected Bond Lengths [Å] and Angles [deg] for Complex **3**·$2H_2O$

Ni(1)−O(21)	2.037(7)
Ni(1)−N(5)	2.069(9)
Ni(1)−O(100)	2.077(8)
Ni(1)−N(15)	2.077(8)
Ni(1)−N(2)	2.081(8)
Ni(1)−N(12)	2.157(8)
Ni(2)−N(35)	2.055(8)
Ni(2)−N(42)	2.070(9)
Ni(2)−N(22)	2.075(9)
Ni(2)−N(45)	2.100(11)
Ni(2)−N(32)	2.120(8)
Ni(2)−N(25)	2.127(8)
Ni(3)−O(1)	2.021(6)
Ni(3)−O(61)	2.022(6)
Ni(3)−O(21)	2.036(6)
Ni(3)−O(51)	2.038(7)
Ni(3)−O(41)	2.040(7)
Ni(3)−O(31)	2.121(6)
Ni(4)−N(65)	2.016(9)
Ni(4)−O(61)	2.017(6)
Ni(4)−N(55)	2.082(9)
Ni(4)−N(52)	2.087(8)
Ni(4)−O(400)	2.124(7)
Ni(4)−O(410)	2.145(8)
Ni(5)−O(81)	2.023(7)
Ni(5)−O(71)	2.045(6)
Ni(5)−O(91)	2.047(7)
Ni(5)−O(1)	2.073(6)
Ni(5)−N(62)	2.087(8)
Ni(5)−O(31)	2.192(6)
Ni(6)−N(92)	2.060(8)
Ni(6)−N(85)	2.079(7)
Ni(6)−N(72)	2.088(7)
Ni(6)−N(75)	2.096(7)
Ni(6)−N(82)	2.112(9)
Ni(6)−N(95)	2.114(8)
O(21)−Ni(1)−N(5)	163.7(3)
O(21)−Ni(1)−O(100)	85.7(3)
N(5)−Ni(1)−O(100)	96.1(3)
O(21)−Ni(1)−N(15)	95.9(3)
N(5)−Ni(1)−N(15)	100.0(3)
O(100)−Ni(1)−N(15)	97.4(3)
O(21)−Ni(1)−N(2)	83.4(3)
N(5)−Ni(1)−N(2)	80.3(3)
O(100)−Ni(1)−N(2)	91.2(3)
N(15)−Ni(1)−N(2)	171.4(3)
O(21)−Ni(1)−N(12)	88.7(3)
N(5)−Ni(1)−N(12)	90.9(3)
O(100)−Ni(1)−N(12)	172.0(3)
N(15)−Ni(1)−N(12)	77.6(3)
N(2)−Ni(1)−N(12)	93.8(3)
N(35)−Ni(2)−N(42)	164.6(3)
N(35)−Ni(2)−N(22)	101.5(3)
N(42)−Ni(2)−N(22)	88.0(4)
N(35)−Ni(2)−N(45)	94.9(4)
N(42)−Ni(2)−N(45)	78.8(4)
N(22)−Ni(2)−N(45)	159.6(3)
N(35)−Ni(2)−N(32)	78.3(3)
N(42)−Ni(2)−N(32)	90.0(3)
N(22)−Ni(2)−N(32)	88.9(3)
N(45)−Ni(2)−N(32)	106.3(3)
N(35)−Ni(2)−N(25)	99.2(3)
N(42)−Ni(2)−N(25)	94.6(3)
N(22)−Ni(2)−N(25)	77.5(4)
N(45)−Ni(2)−N(25)	88.1(4)
N(32)−Ni(2)−N(25)	165.4(4)
O(1)−Ni(3)−O(61)	84.8(3)
O(1)−Ni(3)−O(21)	87.7(3)
O(61)−Ni(3)−O(21)	172.3(3)
O(1)−Ni(3)−O(51)	93.6(3)
O(61)−Ni(3)−O(51)	93.5(3)
O(21)−Ni(3)−O(51)	85.4(3)
O(1)−Ni(3)−O(41)	172.4(3)
O(61)−Ni(3)−O(41)	87.9(3)
O(21)−Ni(3)−O(41)	99.7(3)
O(51)−Ni(3)−O(41)	89.0(3)

Table 4. Continued

O(1)−Ni(3)−O(31)	83.1(2)
O(61)−Ni(3)−O(31)	85.6(2)
O(21)−Ni(3)−O(31)	95.1(2)
O(51)−Ni(3)−O(31)	176.6(3)
O(41)−Ni(3)−O(31)	94.2(3)
N(65)−Ni(4)−O(61)	86.4(3)
N(65)−Ni(4)−N(55)	106.1(4)
O(61)−Ni(4)−N(55)	167.5(3)
N(65)−Ni(4)−N(52)	174.4(4)
O(61)−Ni(4)−N(52)	88.0(3)
N(55)−Ni(4)−N(52)	79.5(4)
N(65)−Ni(4)−O(400)	92.6(3)
O(61)−Ni(4)−O(400)	87.7(3)
N(55)−Ni(4)−O(400)	92.7(3)
N(52)−Ni(4)−O(400)	86.3(3)
N(65)−Ni(4)−O(410)	88.8(3)
O(61)−Ni(4)−O(410)	91.0(3)
N(55)−Ni(4)−O(410)	88.2(3)
N(52)−Ni(4)−O(410)	92.2(3)
O(400)−Ni(4)−O(410	178.0(3)
O(81)−Ni(5)−O(71)	94.0(3)
O(81)−Ni(5)−O(91)	94.6(3)
O(71)−Ni(5)−O(91)	97.1(3)
O(81)−Ni(5)−O(1)	175.8(3)
O(71)−Ni(5)−O(1)	86.9(2)
O(91)−Ni(5)−O(1)	89.3(3)
O(81)−Ni(5)−N(62)	93.9(3)
O(71)−Ni(5)−N(62)	171.1(3)
O(91)−Ni(5)−N(62)	86.6(3)
O(1)−Ni(5)−N(62)	85.0(3)
O(81)−Ni(5)−O(31)	95.7(3)
O(71)−Ni(5)−O(31)	96.9(2)
O(91)−Ni(5)−O(31)	162.0(2)
O(1)−Ni(5)−O(31)	80.1(2)
N(62)−Ni(5)−O(31)	78.1(3)
N(92)−Ni(6)−N(85)	100.6(3)
N(92)−Ni(6)−N(72)	90.9(3)
N(85)−Ni(6)−N(72)	161.8(3)
N(92)−Ni(6)−N(75)	160.5(3)
N(85)−Ni(6)−N(75)	94.3(3)
N(72)−Ni(6)−N(75)	78.1(3)
N(92)−Ni(6)−N(82)	86.4(3)
N(85)−Ni(6)−N(82)	79.1(3)
N(72)−Ni(6)−N(82)	87.6(3)
N(75)−Ni(6)−N(82)	108.9(3)
N(92)−Ni(6)−N(95)	77.8(3)
N(85)−Ni(6)−N(95)	91.6(3)
N(72)−Ni(6)−N(95)	104.7(3)
N(75)−Ni(6)−N(95)	89.3(3)
N(82)−Ni(6)−N(95)	160.0(3)
Ni(3)−O(1)−Ni(5)	96.5(3)
Ni(3)−O(21)−Ni(1)	120.7(3)
Ni(3)−O(31)−Ni(5)	90.2(2)
Ni(4)−O(61)−Ni(3)	115.6(3)

Magnetic Properties

The magnetic susceptibility data for a dried and powdered sample of complex **1**, which did not lose its coordinated methanol, as checked by different spectroscopic methods, were collected at an applied magnetic field of 1 T to be in the linear range and in the temperature range 2−290 K. A plot of the effective magnetic moment, μ_{eff}, versus the temperature, T, is displayed in Figure 6. The effective magnetic moment, μ_{eff}, decreases monotonically from 6.18 μ_B ($\chi_{mol}T = 4.773$ cm^3 K mol^{-1}) at 290 K upon cooling to 3.04 μ_B ($\chi_{mol}T = 1.55$ cm^3 K mol^{-1}) at 5 K, indicating the presence of dominating antiferromagnetic exchange coupling between the paramagnetic centers in **1**. Below 5 K, μ_{eff} drops to 1.854 μ_B ($\chi_{mol}T = 0.4297$ cm^3 K mol^{-1}) at 2 K due to the combined effects of field saturation and zero-field splitting.

Table 5. Selected Bond Lengths [Å] and Angles [deg] for Complex **4**·3CH$_3$CN[a]

Ni(1)−N(32)	1.826(2)
Ni(1)−O(30)	1.848(3)
Ni(1)−O(30X)	1.866(4)
Ni(1)−O(1)	1.8688(18)
Ni(1)−N(35)	1.886(2)
Ni(2)−N(2)	1.829(2)
Ni(2)−O(30)	1.837(3)
Ni(2)−O(18)#1	1.8569(18)
Ni(2)−O(30X)	1.862(4)
Ni(2)−N(5)	1.866(2)
Ni(3)−N(17)#1	1.825(2)
Ni(3)−O(30X)	1.841(4)
Ni(3)−O(31)	1.848(2)
Ni(3)−O(30)	1.869(3)
Ni(3)−N(14)#1	1.876(2)
N(32)−Ni(1)−O(30)	90.67(12)
N(32)−Ni(1)−O(30X)	88.53(13)
O(30)−Ni(1)−O(30X)	32.06(15)
N(32)−Ni(1)−O(1)	173.94(11)
O(30)−Ni(1)−O(1)	93.43(11)
O(30X)-Ni(1)−O(1)	92.57(13)
N(32)−Ni(1)−N(35)	82.55(10)
O(30)−Ni(1)−N(35)	162.40(13)
O(30X)−Ni(1)−N(35)	161.96(15)
O(1)−Ni(1)−N(35)	94.75(9)
N(2)−Ni(2)−O(30)	91.11(12)
N(2)−Ni(2)−O(18)#1	174.37(10)
O(30)−Ni(2)−O(18)#1	93.40(11)
N(2)−Ni(2)−O(30X)	89.48(13)
O(30)−Ni(2)−O(30X)	32.19(15)
O(18)#1−Ni(2)−O(30X)	92.55(13)
N(2)−Ni(2)−N(5)	83.34(9)
O(30)−Ni(2)−N(5)	163.35(13)
O(18)#1−Ni(2)−N(5)	93.21(9)
O(30X)−Ni(2)−N(5)	162.12(15)
N(17)#1−Ni(3)−O(30X)	89.31(14)
N(17)#1−Ni(3)−O(31)	174.37(11)
O(30X)−Ni(3)−O(31)	92.37(13)
N(17)#1−Ni(3)−O(30)	90.48(12)
O(30X)−Ni(3)−O(30)	32.10(15)
O(31)−Ni(3)−O(30)	93.80(11)
N(17)#1−Ni(3)−N(14)#1	83.11(9)
O(30X)−Ni(3)−N(14)#1	161.30(16)
O(31)−Ni(3)−N(14)#1	93.68(9)
O(30)−Ni(3)−N(14)#1	163.78(13)
Ni(2)−O(30)−Ni(1)	113.59(17)
Ni(2)−O(30)−Ni(3)	112.58(17)
Ni(1)−O(30)−Ni(3)	112.45(17)
Ni(3)−O(30X)−Ni(2)	112.7(2)
Ni(3)−O(30X)−Ni(1)	112.9(2)
Ni(2)−-O(30X)−Ni(1)	111.7(2)

[a]Symmetry transformations used to generate equivalent atoms #1: $-x + 1, y, -z - 1/2$.

To avoid overparametrization, we have considered a "two-J" model (Scheme 2) in which the interactions between the atoms Ni(1)/Ni(2) and Ni(3)/Ni(4) propagated via the phenoxide and acetate bridging groups are taken to be equal and represented by J_1, whereas J_2 represents the exchange interaction between the Ni(2)/Ni(3) atoms propagated via the singly bridging oximate ligand, Ni(2)−N(25)−O(26)−Ni(3). The susceptibility data based on the Heisenberg spin Hamiltonian for a tetranuclear complex were simulated, shown as the solid line in Figure 6, using a least-squares-fitting computer program with a full-matrix diagonalization method.[29]

$$\hat{H} = -2J_1 \cdot (\hat{S}_1 \cdot \hat{S}_2 + \hat{S}_3 \cdot \hat{S}_4) - 2J_2(\hat{S}_2 \cdot \hat{S}_3)$$

(29) Bill, E. *Julx Program*; Max-Planck-Institut für Bioanorganische Chemie: Mülheim an der Ruhr, Germany, 2005.

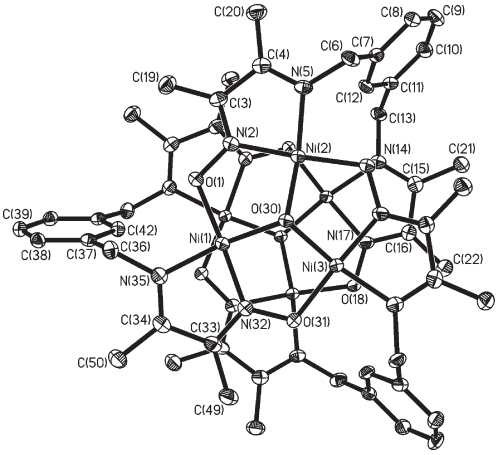

Figure 5. Molecular structure of the dication in complex **4**, Ni^{II}_6.

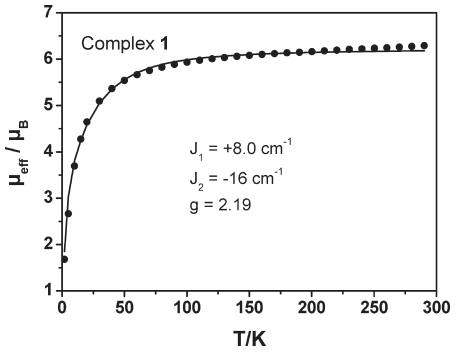

Figure 6. Plot of the effective magnetic moment, μ_{eff}, for complex **1** as a function of temperature (T). The solid line represents the best fit with the full-diagonalization matrix method using the parameters given in the text.

with

$$S_1 = S_2 = S_3 = S_4 = S_{Ni} = 1$$

The best fit parameters obtained are $J_1 = +8.0$ cm^{-1}, $J_2 = -16.0$ cm^{-1}, and $g = 2.19$. No other parameters had to be invoked to obtain the simulation shown as the solid line in Figure 6. However, to be sure about possible covariances of J_1 and J_2, we calculated a two-dimensional error surface as a function of the two parameters. The result, shown as a contour plot in Figure 7, nicely demonstrates the true global solution and rules out the presence of other local minima. The 3D plot is also depicted in Figure 7. The range of confidence for the exchange coupling constants is thus safely estimated to be $J_1 = +8.0$ (± 0.2) cm^{-1} and $J_2 = -16.0$ (± 0.2) cm^{-1}.

The ferromagnetic interaction, $J_1 = +8.0$ cm^{-1}, should be associated with the exchange interactions involving heterobridged, diphenoxide-monocarboxylate dinickel(II) Ni(1)/Ni(2) and Ni(3)/Ni(4) units in **1**. As the axial exchange pathways through the carboxylate bridges in such dinickel (II) complexes with equatorial $Ni_2(O_{phenoxide})_2$ cores are very weak antiferromagnetically and insignificant[30] in comparison to spin exchange through the Ni−O(phenoxide)−Ni paths,[26] the most important parameter in determining the nature and magnitude of exchange interactions in such

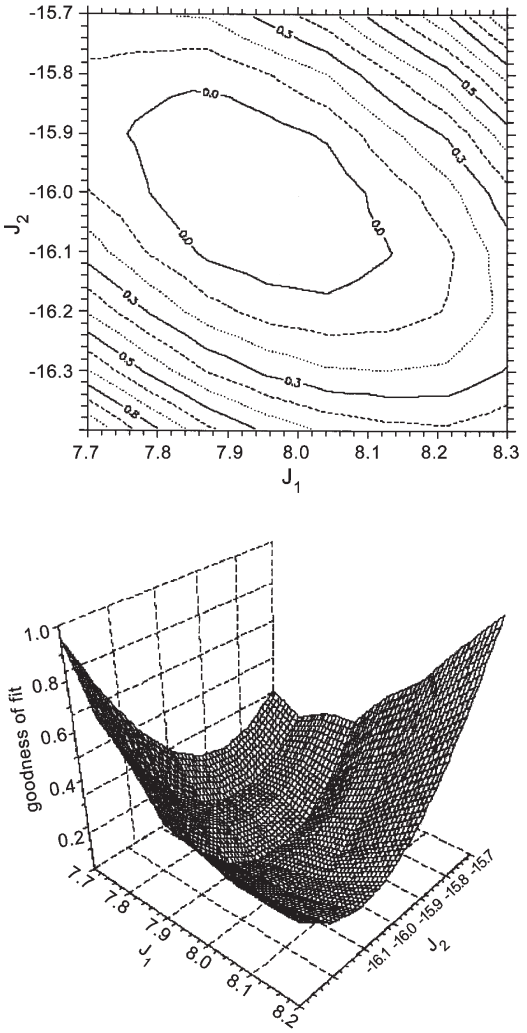

Figure 7. 2D- and 3D-contour projections of the relative error surface for fitting the magnetic data of complex **1**.

heterobridged dinickel(II) complexes is Ni−O−Ni angles. A ferromagnetic exchange interaction is observed when this angle is close to orthogonality. On the other hand, Ni−O−Ni angles[31] in the vicinity of and larger than 97° lead to an antiferromagnetic interaction. Thus, the ferromagnetic coupling, $J_1 = +8.0$ cm^{-1}, may be attributed to the Ni−O-(phenoxide)−Ni angles, lying in a small range, 93.7(1)−94.8(1)°, in complex **1**. It is noteworthy in this connection that Ni(1)···Ni(2) at 2.921 Å and Ni(3)···Ni(4) at 2.950 Å distances are shorter than that commonly observed and in accord with the above rationale.

In agreement with the above notion are also the observations of nonplanarity of the phenoxide-bridging networks Ni_2O_2 and considerably shorter Ni−O(phenoxide) distances relative to those of other comparable complexes.[20,25]

To date, structurally characterized oximato-bridged homometal nickel(II) complexes, which have been subjected to magnetic susceptibility measurements to evaluate the nature of exchange coupling, are limited and exhibit antiferromagnetic exchange coupling constants lying between $J = -7$ and -80 cm^{-1}. Although **1** is the only known monooximato-bridged nickel(II) complex, the observed antiferromagnetic

(30) (a) Chaudhuri, P.; Küppers, H.-J.; Wieghardt, K.; Gehring, S.; Haase, W.; Nuber, B.; Weiss, J. *J. Chem. Soc., Dalton Trans.* **1988**, 1367. (b) Turpeinen, U.; Hämälainen, R.; Reedijk, J. *Polyhedron* **1987**, 6.

(31) Nanda, K. K.; Thompson, L. K.; Bridson, J. N.; Nag, K. *J. Chem. Soc., Chem. Commun.* **1994**, 1337.

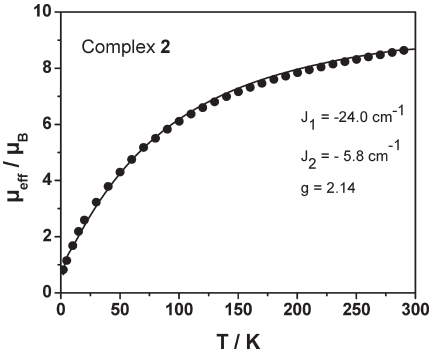

Figure 8. Plot of μ_{eff} vs T for complex **2**. The solid line represents the best least-squares fit parameters given in the text.

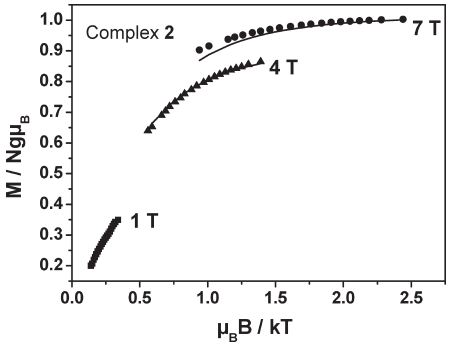

Figure 9. Plot of VTVH measurements for complex **2**. The solid lines represent the best fit parameters given in the text.

Scheme 2

$$\mathbf{Ni(1)} \overset{J_1}{\longleftrightarrow} \mathbf{Ni(2)} \overset{J_2}{\longleftrightarrow} \mathbf{Ni(3)} \overset{J_1}{\longleftrightarrow} \mathbf{Ni(4)}$$

interaction, $J_2 = -16.0$ cm^{-1}, lies well within the range reported in the literature. We note that the monobridging oximato mode, Ni(3)−O(26)−N(25)−Ni(2), is not planar and is comparable with that in $[LNi^{II}(PyA\text{-}Ph)_3Ni^{II}]^+$, described earlier by us,[17] exhibiting $J = -59.4$ cm^{-1}. Considering that $[LNi^{II}(PyA\text{-}Ph)_3Ni^{II}]^+$ contains three oximato (−N−O) bridges, the magnitude of the antiferromagnetic interaction, $J_2 = -16.0$ cm^{-1}, mediated by a single NO bridge in **1** is quite reasonable.

The magnetic susceptibility data for polycrystalline samples of **2** are displayed in Figure 8 as a plot of the magnetic moment (μ_{eff}) versus the temperature (T). The effective magnetic moment of $\mu_{eff} = 8.31$ μ_B ($\chi_{mol}T = 8.634$ cm^3 mol^{-1} K) for **2** at 290 K is smaller than the spin-only value expected for nine isolated Ni(II) ions of $\mu_{eff} = 8.49$ μ_B with $g_{Ni} = 2.0$, indicating an overall antiferromagnetic spin coupling between the Ni(II) centers. Accordingly, the magnetic moment decreases monotonically with a lowering of the temperature, reaching a value of $\mu_{eff} = 2.56$ μ_B ($\chi_{mol}T = 0.8203$ cm^3 mol^{-1} K) at 2 K.

The exchange-coupling model shown in Scheme 3 was considered for simulation of the experimental magnetic data using the irreducible tensor operator approach[32] with the Heisenberg Hamiltonian in the form of $\hat{H} = -2J\hat{S}_i \cdot \hat{S}_j$. As it is not possible to simulate the experimental data with a single coupling constant that takes into account all of the exchange pathways being equal, we have used the next simplest model, namely, a two-J model, with the consideration that a diatomic oximate bridge, μ-(ON) [Ni−O−N−Ni], is expected to provide the main superexchange σ pathway, and this interaction is stronger than that mediated through the μ_3-oximate oxygen, [Ni−O(Ni)−N−Ni, μ_3-ON]. We had also in mind that the μ_2- and μ_3-OH groups and the aqua bridges (μ_2 -OH $_2$) are very weak exchange mediators for the nickel centers. [30]

The best fit parameters obtained from the simulation shown as the solid line in Figure 8 are $J_1 = -24.0$ cm^{-1}, $J_2 = -5.8$ cm^{-1}, with $g = 2.14$, where J_1 represents interactions mediated by a diatomic oximate, μ_2-NO, bridge and μ_2- or μ_3-OH groups, whereas the J_2 interaction is transmitted through a μ_3-oximate and a μ_3-OH group. These moderate coupling constants, J_1 and J_2, are consistent with those reported for oximate-bridged Ni(II) complexes.[7,17−19] A single-atom oximate μ_3-O bridges three metal centers, thus increasing the

(32) Gatteschi, D.; Pardi, L. *Gazz. Chim. Ital.* **1993**, *123*, 231.

Scheme 3

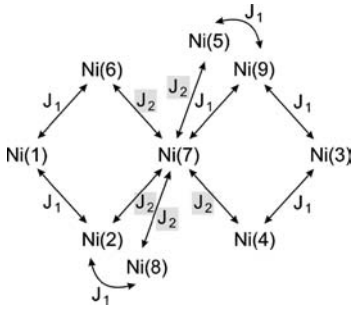

Ni−O_{ox} bond lengths in comparison to those for the oximate μ_2-O-bridge and hence resulting in a diminution of the strength of antiferromagnetic exchange coupling as is observed for protonation or metalation of the μ_2-oxo bridge. Hence, the strength of the J_1 interaction representing primarily coupling mediation by the two-atom N−O linkage is stronger than the J_2 interaction mediated mainly through the single-atom μ_3-oximate oxygen, which is in accord with the corresponding literature values. Analysis of the spin energy levels indicates an $S_t = 1.0$ ground state, in good agreement with the magnetization experiments.

Complex **2** possesses an $S_t = 1.0$ ground state, which has been confirmed by the variable-field (1, 4, and 7 T) and variable-temperature (2−5 K) magnetization (VTVH) measurements (Figure 9). From the best fit with a fixed $S = 1.0$, we have evaluated the zero-field splitting parameter D to be $D_{S=1} = -6.3$ cm^{-1} with $g = 2.18$. We want to stress that all of our attempts to fit the VTVH measurements with a positive D value failed. One should be careful about the accuracy of the zero-field splitting parameter evaluated from powder magnetic susceptibility measurements.

At this point, a brief comparison of **2** with the enneanuclear nickel(II) cation of pyridine-2-aldoxime[15] (Scheme 1) containing identical Ni−ligand connectivity is warranted. That the imidazole-N's are weaker σ donors than the pyridine-N's is reflected in the weakness of the J_1 and J_2 interactions for **2**; this notion is further strengthened by a comparison of the corresponding Ni−N bond lengths. As expected, both compounds possess an $S_t = 1.0$ ground state, but with the zero-field splitting parameters of opposite sign.

The μ_{eff} for **3** steadily decreases from 5.483 μ_B ($\chi_{mol}T = 3.759$ cm^3 mol^{-1} K) at 290 K to a value of $\mu_{eff} = 2.361$ μ_B ($\chi_{mol}T = 0.6970$ cm^3 mol^{-1} K) at 5 K, which then further decreases to 2.069 μ_B ($\chi_{mol}T = 0.5352$ cm^3 mol^{-1} K) at 2 K

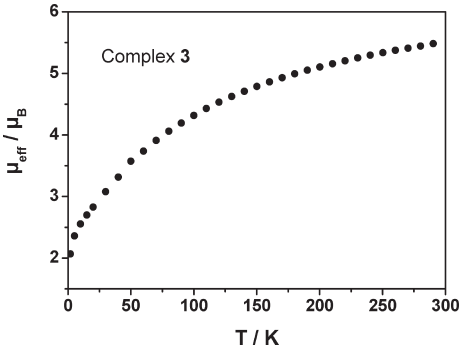

Figure 10. Plot of the effective magnetic moment μ_{eff} as a function of temperature (T) for complex **3**.

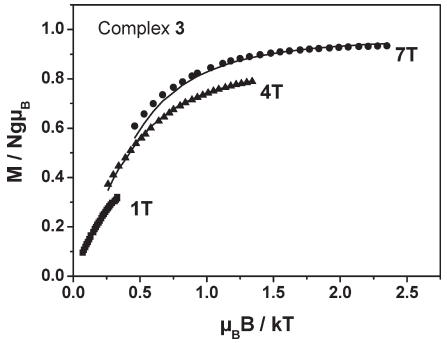

Figure 11. Plot of reduced magnetization vs $\mu_B B/kT$ for complex **3** in the temperature range 2−10 K. Solid lines are the fits of the data with the parameters given in the text.

(Figure 10). The 290 K value is much less than the spin-only (g = 2.0) value of μ_{eff} = 6.932 μ_B for six noninteracting Ni^{II} ions, indicating the presence of dominant antiferromagnetic exchange interactions. Given the size and low-symmetry of the Ni_6 cation, and the resulting number of inequivalent exchange constants, it is not possible to apply the Kambe method[33] to determine the individual pairwise Ni_2 exchange parameters, and we concentrated instead on characterizing the ground state spin, S_{total} (S_t), and the zero-field splitting parameter, D.

To probe the spin ground state S_t of complex **3**, magnetization data were collected at 1, 4, and 7 T in the temperature range 2−10 K (∼27 points). The resulting data for **3** are shown in Figure 11 as a reduced magnetization $M/Ng\mu_B$ versus $\mu_B B/kT$, where M is the magnetization, N is Avogadro's number, μ_B is the Bohr magneton, B is the magnetic field strength, and k is Boltzmann's constant. For a system occupying only the ground state and experiencing no zero-field splitting (D), the various isofield lines would superimpose on each other and saturate at a value of total spin S_t. The curves (Figure 11) show decent nesting as a function of the field, which provides sensitive information on the parameter D. The nonsuperposition of the VTVH plots indicates the presence of many thermally accessible S states or the presence of zero-field splitting. The VTVH measurements yield a ground state S_t = 1.0

The experimental magnetic data were analyzed on the basis of the spin-Hamiltonian

$$\hat{H}_z = D\hat{S}_z^2 + g\mu_B\hat{S}_z B$$

in which $\hat{S}$, g, and D are the single-ion spin operators, g factors, and axial single-ion zero-field splitting parameter, respectively. The best fit is shown as the solid line in Figure 11 and was obtained with S_t = 1.0 (fixed), g = 2.10, and $D_{S=1}$ = −7.2 cm^{-1}. With a positive D value, no reasonable simulation of the VTVH data was obtained. The D value should be taken with care.

Complex **4** is diamagnetic, bearing testimony to the presence of square-planar Ni(II) centers, each with low-spin d^8 electron configuration.

Concluding Remarks and Outlook

We report a new binucleating ligand incorporating N_4O_2 donor atoms and providing additionally oxime functionality, together with two other already reported oxime-containing ligands, which can yield polynuclear oximate-bridged complexes. Crystallographic bond parameters and spectral and magnetic properties were collectively used to determine the electronic structures of the nickel(II) complexes, Ni^{II}_4, Ni^{II}_6, and Ni^{II}_9 species, synthesized. The new oxime-containing binucleating ligand (H_4L^1) yields an interesting tetranickel(II) species, which is a dimer of Ni^{II}_2 units connected by a rare single two-atom (N−O) oximate bridge, thus making evaluation of exchange interactions mediated through such a single (−N−O−) bridge feasible. Moderate antiferromagnetic exchange interactions, as expected, have been established from the variable-temperature magnetic susceptibility measurements between the paramagnetic nickel(II) (S_{Ni} = 1) centers. Fulfilling our expectation, the ligand HL^2 (1-methylimidazole-2-aldoxime, Scheme 1) results in a nonanuclear Ni(II) complex, whose atom connectivity is identical to that in the Ni^{II}_9 species[15] isolated earlier by us with the very similar ligand pyridine-2-aldoxime, HPyA (Scheme 1), and thus opening up an interesting opportunity for comparison between pyridine-N and imidazole-N as σ-donor atoms. The imidazole-N's are weaker donor ligands in comparison to the pyridine-N's, as evidenced not only by the bond parameters but also by weaker antiferromagnetic interactions exhibited by the HL^2-containing compounds. In addition to the Ni^{II}_9 species (complex **2**), a hexanuclear species, Ni^{II}_6, (complex **3**) is available to the Ni(II)−oxime series under a slightly different reaction condition, thus indicating the possibility of developing a rich chemistry for HL^2, like that for existing chemistry with HPyA. We have already reported such dinickel(II) complexes for comparison purposes.[17] The ligand H_2L^3 has not yet yielded, as here reported, any interesting magnetic material, but its further use with a coligand might induce a change in the coordination number of four to six for nickel(II) centers; however, the structural data for the $[Ni^{II}_3(\mu_3\text{-}O)]^{4-}$ units now available are noteworthy. A noteworthy point is that none of the compounds, albeit their oligonuclearity, has resulted in high-spin ground states.

In essence, the reported complexes, Ni^{II}_4, Ni^{II}_6, and Ni^{II}_9, are an interesting addition to the Ni(II)−oxime series and suggest a future direction for producing more polynuclear complexes based on new ligands containing oxime functionality.

(33) Kambe, J. K. *J. Phys. Soc. Jpn.* **1950**, *5*, 48.

Acknowledgment. Financial support from the Max-Planck Society and German Research Council (Deutsche Forschungsgemeinschaft) is gratefully acknowledged (Priority Program "Molecular Magnetism"). The skilful technical assistance of H. Schucht and A. Goebels is thankfully acknowledged. The involvement of Dr. S. Khanra at the initial stage of the project is highly appreciated.

Supporting Information Available: Crystallographic CIF files for **1**−**4** and Table S1 listing hydrogen-bonded distances in **1**. This material is available free of charge via the Internet at http://pubs.acs.org.